

Master's thesis

**Activin-A, Myostatin and Interleukin-6 in Cancer
Associated Cachexia**

Jouni Härkönen



University of Jyväskylä

Department of Biological and Environmental Science

Cell and Molecular Biology

9.3.2017

PREFACE

This work was conducted at the laboratory premises of The Department of Health Sciences, University of Jyväskylä, during the year 2016.

Firstly, I wish to thank my primary thesis supervisor Juha Hulmi for his helpful remarks as well as his flexibility and supportive approach, and for giving me the opportunity to contribute in such an interesting topic. I would also like to express my thanks to Satu Pekkala, Mika Silvennoinen, Tuuli Nissinen and Jaakko Hentilä for their input in technical assistance during this work. In addition, I would like to thank my co-supervisor Janne Ihalainen for reviewing my thesis. Finally, I express my gratitude towards my family and friends, who have provided me an invaluable supportive social environment, making all this work possible and enjoyable.

Kuopio, February 2017

Jouni Härkönen

Tekijä: Jouni Härkönen
Tutkielman nimi: Aktiviini-A, Myostatiini ja Interleukiini-6 syövän aiheuttamassa lihaskadossa
English title: Activin-A, Myostatin and Interleukin-6 in Cancer Associated Cachexia
Päivämäärä: 09.03.2017 **Sivumäärä:** 37+4

Laitos: Bio- ja ympäristötieteiden laitos
Oppiaine: Solu- and Molekyylibiologia
Tutkielman ohjaaja(t): Juha Hulmi

Tiivistelmä:

Kakeksia on lihaskudosta kuluttava kroonisiin sairauksiin liittyvä patologinen tila, jota esiintyy esimerkiksi syövässä, diabeteksessa ja AIDS:ssa. Noin 80 %:lla syöpäpotilaista esiintyy kakeksian oireita, ja noin 25 %:a syöpäkuolleisuudesta voidaan yhdistää tähän. Kakeksiaa ilmentävillä potilailla ja koe-eläimillä esiintyy verenkierrassa sytokiinejä ja TGF- β –proteiiniperheen molekyylejä, kuten interleukiini-6:sta, myostatiinia ja aktiviini-A:ta. Näiden viestiaineiden mekanistista roolia kakeksiassa ei ole vielä täysin selvitetty. Tässä työssä tutkittiin edellä mainittujen viestiaineiden geeniekspressiota käänteistranskriptio-PCR:llä kakeksiaa aiheuttavista tuumoreista sekä kakeksiaa ilmentävästä lihaskudoksesta. Näiden analyysien tarkoitus on selvittää ovatko kyseiset merkkiaineet pääosin peräisin tuumorista vai lihaskudoksesta. Lisäksi tässä työssä optimoitiin CAGA-lusiferaasiplasmiditransfektio C2C12-myoblastisoluille. Tätä geenikonstruktia voidaan hyödyntää tutkittaessa TGF- β proteiinien vaikutusta aktiviinireseptori 2B –välitteiseen signaalointiin. Konstruktin toimintaa testattiin lisäksi aktivoimalla signaalinvälitysreittiä eksogeenisellä Aktiviini-A:lla, ja estämällä tätä liukoosella aktiviinireseptorilla. Tämä tutkielma osoittaa että aktiviini-A:n ja interleukiini-6:en ekspresiotasot ovat merkittävästi koholla kakeettisessa C26 tuumorissa, ja aktiviini-A:n ekspresio on alentunut kakeksiaa ilmentävässä lihaksessa. Lisäksi työssä esitetään toimiva, optimoitu plasmiditransfektioprotokolla yleisesti hankalasti transfektoituvalle C2C12-solulinjalle. Edellä mainittua transfektiota voidaan hyödyntää tutkittaessa kakeksiaa aiheuttavien TGF- β –proteiinien vaikutusta lihaskudokseen. Tällaisilla *in vitro* –menetelmillä voidaan osittain korvata ja tukea aiheeseen liittyvää eläinkokeilla tehtävää tutkimusta.

Avainsanat: Kakeksia, Aktiviini-A, Myostatiini, Interleukiini-6, C2C12

Author: Jouni Härkönen
Title of thesis: Activin-A, Myostatin and Interleukin-6 in Cancer Associated Cachexia
Finnish title: Aktiviini-A, Myostatiini ja Interleukiini-6 syövän aiheuttamassa lihaskadossa
Date: 09.03.2017 **Pages:** 37+4
Department: Department of Biological and Environmental Science
Chair: Cell and Molecular Biology
Supervisor(s): Juha Hulmi

Abstract:

Cachexia is a muscle wasting condition associated with multiple different chronic illnesses, such as cancer, diabetes and AIDS. In cancer, approximately 80% of patients with advanced disease have symptoms of muscle wasting, and around 25% of cancer mortality concerns cachexia. Elevated serum levels of different cytokines and TGF- β protein family members, such as Interleukin-6, Myostatin and Activin-A, have been observed in cachectic patients and test animals. However, the mechanistic role and the relative contribution of these molecules to muscle loss in the syndrome have not yet been fully elucidated. In this thesis, the gene-expression levels of Activin-A, Myostatin and Interleukin-6 was assessed with Reverse-Transcriptase quantitative PCR from the tumor and muscle tissue of cachectic C26-tumor-bearing mice to clarify whether they arise from the tumor or are muscle derived. Additionally, transfection of CAGA-luciferase plasmid construct was optimized for the C2C12 murine myoblast cell-line to be utilized in research concerning TGF- β mediated cancer-associated cachexia *in vitro*. The function of the construct was tested by administration of exogenous Activin-A, with and without its inhibitor, into the C2C12 growth media. This thesis showed a marked increase in the expression levels of Activin-A (inhibin- β A) and IL-6 mRNA in cachexia inducing tumors (C26) when compared to tumors not inducing cachexia (Lewis-Lung-Cancer) ($P < 0.001$). Additionally, the results show decrease in muscle-derived Activin-A (inhibin- β A) in the cachectic groups ($P < 0.05$). These results imply that Activin-A and Interleukin-6 are strongly induced in the tumors that produced cachexia *in vivo*. This work also presents a successful, optimized plasmid transfection protocol for the notoriously transfection resistant C2C12-myoblast cell line. The presented *in vitro* -method can partially replace animal tests in related settings, when studying the mechanistic effects of cachexia-inducing TGF- β proteins on muscle tissue.

Keywords: Cachexia, Myostatin, Activin-A, Interleukin-6, C2C12

TABLE OF CONTENTS

PREFACE	1
ABBREVIATIONS	7
1. INTRODUCTION.....	8
1.1 Overview of cancer-associated cachexia.....	8
1.2 Activin-A.....	9
1.3 Myostatin.....	10
1.4 Interleukin-6	11
1.5 Characteristics of the C26, LLC and C2C12 cell lines.....	12
2. AIMS OF THE STUDY	13
3. MATERIALS & METHODS.....	15
3.1 Gene expression assessment.....	15
3.1.1 Details on the animal experiments.....	15
3.1.2 Primer design and testing	15
3.1.2 Tissue lysis, RNA-extraction and gene expression analysis	16
3.1.3 RT-qPCR data analysis	17
3.2 C2C12 myoblast cell experiments	18
3.2.1 Thawing and cultivation of C2C12 cells	18
3.2.2 Optimization of C2C12 transfection.....	18
3.2.2.1 Transfection with Lipofectamine 3000 and Fugene 6	18
3.2.2.2 Optimization of Lipofectamine 3000 transfection	20
3.2.2.3 Further optimization of Lipofectamine 3000 transfection.....	21
3.2.3 Exposure to Activin-A and ACVR2B	21
3.2.3.1 Activin-A exposure.....	21
3.2.3.2 ACVR2B ligand blockade	21
3.3 Statistical analysis.....	21
4. RESULTS	23
4.1 Basic characteristics of the tumour-bearing mice	23
4.2 Relative expression levels in tumor	23
4.3 Relative expression levels in muscle	24
4.4 Lipofectamine 3000 and Fugene 6 Reagents in C2C12 Transfection.....	24

4.5 Optimization of Lipofectamine 3000 transfection.....	25
4.6 Activin-A exposure and blockade.....	26
5. DISCUSSION.....	28
5.1 Tumor and muscle gene expression levels.....	28
5.2 Optimization of C2C12 transfection.....	31
5.3 C2C12 ActA exposure and blockade.....	33
REFERENCES.....	34
SUPPLEMENTARY DATA.....	38

ABBREVIATIONS

ActA	Activin-A
ACVR2B	Activin-receptor II beta
CAC	Cancer-associated cachexia
Ct	Cycle threshold
C2C12	C2C12 murine myoblast cell line
C26	C26 colon carcinoma
LLC	Lewis-Lung-Cancer
Mstn	Myostatin
RT-qPCR	Reverse Transcriptase quantitative polymerase chain reaction
sACVR2B	Soluble Activin-receptor II beta
TGF- β	Transcription Growth Factor β

1. INTRODUCTION

1.1 Overview of cancer-associated cachexia

Cachexia is a pathological condition characterized by ongoing skeletal muscle wasting, which is usually accompanied with adipose tissue loss. It is associated with many chronic clinical conditions, such as diabetes, AIDS and cancer. In cancer, cachexia notably reduces patient quality of life, treatment tolerability and survival. Up to 80 % of cancer patients with advanced malignancy experience muscle wasting, and around 25 % of cancer associated mortality concerns cachexia (Tisdale, 2009). Despite this, all current treatment options for cachexia are regarded as palliative care (Aoyagi et. al., 2015). One prominent drug treatment is, however, underway: Anamorelin recently passed two randomized, double-blind phase 3 clinical trials and is currently in preregistration (Temel et. al., 2016).

Cancer-associated cachexia (CAC) is a complex multifactorial syndrome, which is caused by reduced nutritional intake and metabolic factors (Maddocks et. al., 2016). Reduced nutritional intake in cancer is itself multifactorial, involving loss of appetite, impaired gastrointestinal function, fatigue, pain and dysphagia (Tan et. al., 2014). However, CAC cannot be fully reversed with increased nutritional support, which is suggestive to the fact that metabolic components are involved (Fearon et. al., 2011). The metabolic factors of CAC involve e.g. increased systemic inflammation, increased protein catabolism and carbohydrate intolerance (Petruzzelli and Wagner, 2016). Increased serum levels of proinflammatory cytokines and myokines are indeed present in cachectic patients and test animals. These circulating markers include tumor necrosis factor α , Interleukin-1, Interleukin-6 (IL-6), as well as certain transcription growth factor β (TGF- β) protein superfamily members. Interleukin-1 has been linked to increased systemic protein breakdown as well as lipolysis, and IL-6 is mainly associated with body mass and adipose tissue loss. TNF α causes a systemic response, which increases other circulating cytokines. (Petruzzelli and Wagner, 2016) The metabolic component of CAC is mechanistically complex, and circulatory elements involve both host and tumor derived mediators (Petruzzelli and Wagner, 2016; Tsuchida et. al., 2009).

Due to the complexity of the disorder, treatment for CAC has been multimodal, involving nutritional support, increased physical activity and anti-inflammatory drugs (Maddocks et. al., 2016). Regarding the multifactorial nature of CAC, targeting single cytokines with monoclonal antibodies has so far been ineffective in reducing cachectic symptoms (Petruzzelli and Wagner, 2016). Since muscle mass is an independent predictor of patient outcome, directly inhibiting muscle mass wasting is a clinically relevant approach for treatment (Fearon et. al., 2011). Activin-A (ActA) and Myostatin (Mstn) are TGF- β superfamily members known to regulate muscle mass. They are therefore putative mediators of CAC related muscle wasting and potential targets for treatment (Tsuchida et. al., 2009). A recent approach of specifically blocking Activin 2B receptor (ACVR2B), a cell-surface receptor binding multiple TGF- β protein family members including ActA and Mstn, effectively reduced cachectic symptoms and improved survival in cachectic mice allografts (Hatakeyama et. al., 2016). A similar effect was observed with indirect blockade by administration of soluble ACVR2B (sACVR2B) into the bloodstream (Miyamoto et. al., 2016). ACVR2B has affinity for multiple TGF- β superfamily proteins. Thus, its blockade does not pinpoint the treatment effect to a single ligand (Tsuchida et. al., 2009). The independent contributions of Activin-A and Myostatin to CAC have both been studied (Thissen and Loumaye, 2013).

1.2 Activin-A

ActA is a homodimeric protein belonging to the TGF- β superfamily. ActA functions in autocrine, paracrine and endocrine manner, and has a wide set of biological functions. ActA is a known negative regulator of muscle mass, and serum concentration of ActA in CAC has been shown to negatively correlate with body- and lean mass in multiple studies (Thissen and Loumaye, 2013; Chen et. al., 2014; Gilson et. al., 2009). However, the individual contribution of ActA to muscle metabolism has not yet been fully elucidated (Ding et. al., 2016). ActA binds to ACVR2B and increases Smad2/3 transcription factors (Fig. 1). Smad2/3 expression correlates negatively with myofiber diameter in male CD1 mice (Sartori et. al., 2009). However, at least *in vitro*, ACVR2B can mediate muscle catabolism through p38 β mitogen-activated protein

kinase in the case of ActA exposure (Ding et. al., 2016). More research is required to clarify the exact downstream mechanisms in ACVR2B-mediated muscle catabolism in ActA and Mstn exposure.

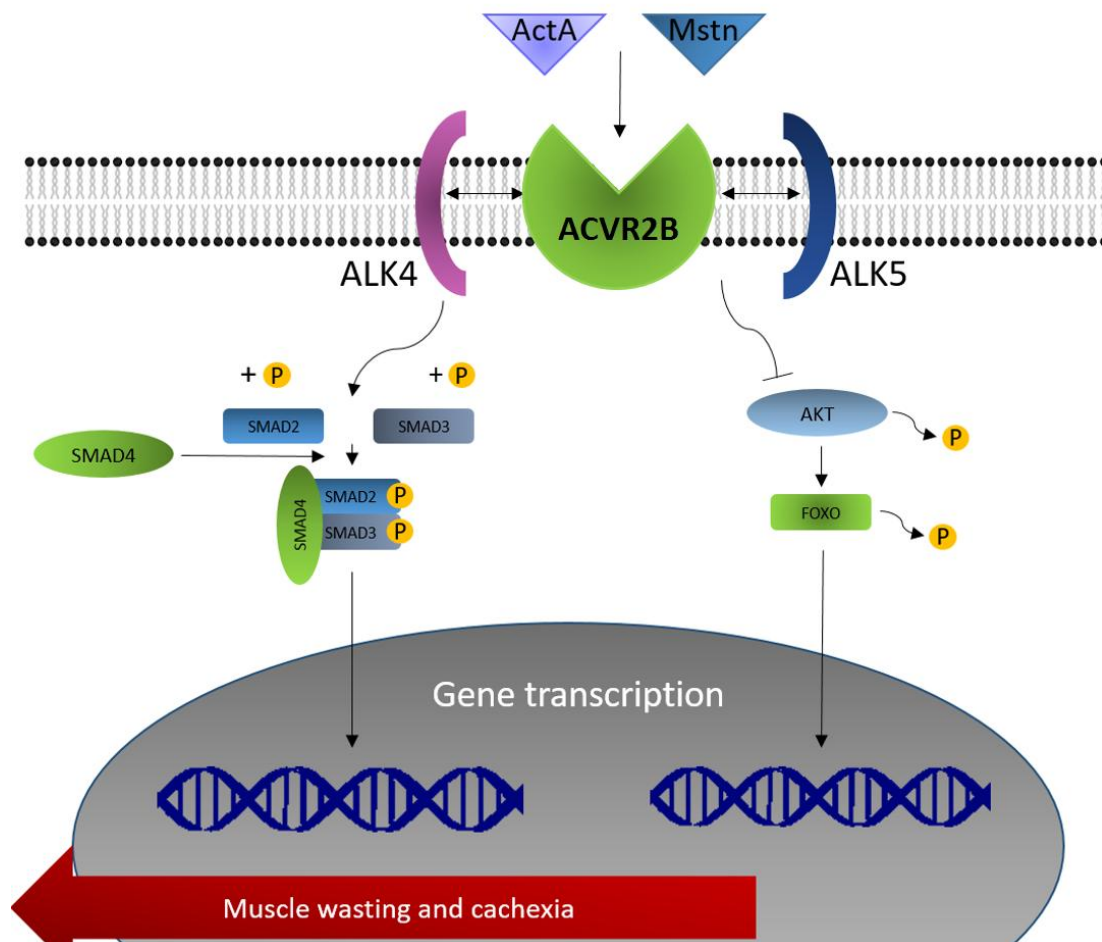


Figure 1: The ACVR2B-pathway. ActA and Mstn have affinity towards ACVR2B. A binding event causes ACVR2B to dimerize, which promotes binding with ALK4 or ALK5. This causes Smad2 and Smad3 phosphorylation and formation of a Smad complex, which activates gene transcription leading to muscle wasting. ActA or Mstn binding also reduces Akt activity. This dephosphorylates FoxO, which activates transcription of different atrogenes that promote muscle protein degradation. (Han et. al., 2013)

1.3 Myostatin

Mstn is also a member of the TGF- β superfamily, and a potent negative regulator of skeletal muscle mass (McPherron et. al., 1997). The effect of Mstn to muscle metabolism is evident in animal knockouts, which express an apparent “double muscled” phenotype of heavy lean mass (Gu et. al., 2016). Conversely, overexpression of Mstn causes skeletal muscle atrophy (Zimmers et. al., 2002). Mstn is mainly

produced in skeletal muscle cells and it regulates muscle mass in paracrine and endocrine manner by down-regulating myogenic signaling molecules, increasing protein degradation and decreasing protein synthesis (Aoyagi et. al., 2015). One prominent mechanism in regarding protein synthesis regulation is inhibition of the Akt/mTOR pathway (Amirouche et. al., 2009). Similar to ActA, Mstn also acts through the ACVR2B-pathway, but its downstream contributors to muscle wasting remain elusive (Sartori et. al., 2009; Aversa et. al., 2012). Nevertheless, ACVR2B-inactive transgenic mice express a muscle hypertrophic phenotype. (Lee and McPherron, 2001) Additionally, Mstn has other mechanisms of action associated with muscle atrophy. (Aversa et. al., 2012) One prominent pathway of Mstn mediated skeletal muscle mass regulation is inhibition of the Akt/mTOR pathway, which controls protein synthesis (Fig. 1) (Amirouche et. al., 2009). Mstn concentration has been shown to be elevated in the circulation of cachectic medullary thyroid cancer patients, which could potentially be utilized in early-stage diagnostic purposes (Hedayati et. al., 2016). However, this observation does not apply to all cachectic cancers, since colorectal and lung cancer patients harbored less circulating Mstn in the cachexia expressing groups (Thissen and Loumaye, 2013). In 2016, Mstn was stated to be abundantly secreted from the cachexia-inducing C26 colon cancer cells in a study that was later retracted for scientific dishonesty, leaving the question unanswered. Consequently, the role of Mstn as a cachectic biomarker requires clarification with further research.

1.4 Interleukin-6

IL-6 is a prominent biomarker in cachexia. It serves as a proinflammatory cytokine when secreted by macrophages and certain cancer types (Fearon et. al., 2012). Circulating IL-6 concentration correlates with loss of body mass as well as reduced amount of adipose tissue, and to some extent contributes to muscle atrophy at least in combination with other cytokines such as ActA (Fearon et. al., 2012; Belizario et. al., 2016; Chen et. al., 2016). A contradictory observation is that IL-6 is also classified as a protective myokine when produced in skeletal muscle (Belizario et. al., 2016). IL-6 expression is elevated after exercise, and satellite cell proliferation as well as migration

is dependent of this expression (Belizario et. al., 2016). However, circulating concentration of IL-6 leading to muscle atrophy has to be supraphysiological to induce an effect, and elevated concentration of IL-6 has also been associated with higher tumor growth rate (Fearon et. al., 2012; Giri et. al., 2001). Thus, increased overall tumor burden and consequent elevated levels of other tumor-derived cachectic factors could explain the loss of skeletal muscle associated with elevated expression level of IL-6.

1.5 Characteristics of the C26, LLC and C2C12 cell lines

C26 colon carcinoma cell line is an undifferentiated Grade IV carcinoma which was originally characterized *in vivo* in the BALB/c mouse strain. (Corbett et. al., 1975) It is highly tumorigenic and has a low potential to metastasize, and exhibits high mortality in inoculated mice. (Sato et. al., 1981) The C26 tumor induces body mass loss and systemic wasting of skeletal muscle and adipose tissue, which are the hallmarks of CAC. Consequently, CAC has been extensively studied with the colon-26 carcinoma (C26) tumor inoculated mice cachexia model. (Bonetto et. al., 2016) The samples used in this study are from a population of C26 tumor-bearing mice, and sACVR2B treatment was applied to one group.

Lewis lung carcinoma (LLC) inoculated tumors were used as non-muscle wasting control tumors in this study. The LLC cell line is originally established by inoculating a primary Lewis lung carcinoma in the lung of a C57BL mouse. The cells are highly tumorigenic and have a low metastatic potential. LLC tumor induces adipose tissue loss but not significant muscle mass wasting in inoculated test animals. (Bertram and Janik, 1980)

The C2C12 murine myoblast cell line is established from C3H mouse muscle satellite cells. C2C12 cells are capable of differentiating rapidly from myoblasts into contractile myotubes with appropriate culturing conditions. (Yaffe and Saxel, 1977) In this thesis, C2C12 myoblast cells were used in the *in vitro* experiments.

2. AIMS OF THE STUDY

The primary aim of this study was to assess the expression levels of cachectic biomarkers, ActA, Mstn and IL-6 in tumor and muscle tissues of cachectic allograft mice. Tumor analyses were conducted for cachexia inducing C26 vs. non-cachectic LLC tumor tissue samples dissected from tumor-bearing mice. Muscle analyses were conducted on the dissected gastrocnemius muscle samples from healthy, C26 tumor bearing untreated and sACVR2B treated groups. These analyses were carried out to assess the relative importance of the aforementioned biomarkers in the relevant tissues.

The secondary aim was to advance the deployment of *in vitro* methods, which could be utilized in studying the effects of ActA, Mstn, and other TGF- β proteins on muscle tissue. The specific aim for this secondary part is to optimize transfection conditions of a Smad-dependent CAGA-luciferase plasmid for C2C12 myoblast cells. The function of the CAGA-luciferase construct is based on Smad2 and Smad3 activation through the ACVR2B pathway (for details on the pathway, see Fig. 1). The construct contains repeats of a Smad3 response element (CAGA) next to luciferase cDNA. Activation of the pathway with e.g. ActA results in Smad phosphorylation, which leads to luciferase transcription through the response element. (Kaivo-Oja et. al., 2005) Accordingly, the Smad-dependent plasmid can be used to monitor the exogenous activity of ActA, Mstn and other TGF- β proteins, which are prominent biomarkers in CAC. An additional aim was to detect a response in luciferase signal in ActA exposure of transfected C2C12-cells, and to inhibit the response with sACVR2B. These conditions are meant to be analogous to the muscle satellite cells of cachectic non-treated and cachectic sACVR2B treated mice, such as in the case of the gene expression experiment in this study. These *in vitro* methods can be used to produce supportive data and partially replace related *in vivo* experiments.

The main research questions in this study were:

1. Is ActA, Mstn and IL-6 expression elevated in cachectic tumors?
2. Is ActA, Mstn and IL-6 expression elevated in the gastrocnemius muscle of tumor-bearing mice?
3. Can the CAGA-luciferase construct be successfully transfected into C2C12 myoblast cells?
4. Does the C2C12 derived luciferase signal increase with exogenous ActA administration?
5. Is the effect of ActA reversed with soluble ACVR2B?

3. MATERIALS & METHODS

3.1 Gene expression assessment

3.1.1 Details on the animal experiments

The mice strain used was BALB/c. Mice were subcutaneously inoculated into upper-back area with 5E5 C26 cells (a gift from Dr. Fabio Penna) or vehicle control, and treated with sACVR2B (5 mg/kg, i.p.) or PBS before and after tumor formation. LLC tumor-samples are from an earlier study conducted by a research-group at the University of Helsinki. Treatment of the animals was in accordance with the European Convention for the Protection of Vertebrate Animals Used for Experimental and Other Scientific Purposes. The protocols were approved by the National Animal Experiment Board. The C26-cancer experiment samples were from two different experiments: tumor samples were obtained from the first experiment when the humane end-point criteria were met, and muscle samples were obtained from a separate experiment where day 11 was predetermined as end-point. The tumours and gastrocnemius muscles were collected after euthanization and analyzed for gene expression.

3.1.2 Primer design and testing

Primers were designed for ActA, Mstn and IL-6 with primer3 software against FASTA-sequences of *Mus musculus Inhba* (ActA), *Mstn* and *Il6* cDNA obtained from the NCBI-website. (Rozen and Skaletsky, 2000) Oligos were checked for specificity with primer-BLAST. (Ye et. al., 2012) The absence of putative secondary structures was screened with OligoAnalyzer 3.1 (<http://eu.idtdna.com/calc/analyzer>); oligos associated with > 10 kcal/mol structures were excluded. The resulting oligos were purchased from Invitrogen (for all sequence information, see supplementary data, *appendix 1*). Primer performance and specificity was tested by conducting qPCR for a dilution series from pooled C26 and LLC tumor cDNA-samples, and assessing product size with agarose gel electrophoresis. Primers with linear standard curves, correct product size and single peaked product melting curves were used in subsequent reverse transcription quantitative polymerase chain reaction (RT-qPCR) analyses. The final primer sequences, including calibrator sequences, Rn18S and 36B4, are presented in

Table 1.

Table 1: Primer sequences for RT-qPCR analyses. Rn18S and 36B4 were used as calibrator genes.

Primer	Sequence (5' → 3')
Mstn_1F	AAGATGGGCTGAATCCCTTT
Mstn_1R	GCAGTCAAGCCCAAAGTCTC
Activin-A_1F	GAACGGGTATGTGGAGATAG
Activin-A_1R	TGAAATAGACGGATGGTGAC
IL-6_1F	ATTCCAGAAACCGCTATGAA
IL-6_1R	CCATTGCACAACCTCTTTTCT
Rn18S_F1	GCAATTATTCCCATGAACG
Rn18S_R1	GGCCTCACTAAACCATCCAA
36B4_F1	GGCCCTGCACTCTCGCTTTC
36B4_R1	TGCCAGGACGCGCTTGT

3.1.2 Tissue lysis, RNA-extraction and gene expression analysis

Tissue lysis, RNA-extraction and RT-qPCR were performed on tissue samples dissected from BALB/c mice. For tumor samples, tumor tissue was dissected for the test group and control group from C26- and LLC-tumor inoculated allograft mice, respectively. Muscle (Gastrocnemius) tissue samples were obtained from three groups: healthy, C26-inoculated untreated and C26-inoculated sACVR2B-treated mice. Tissue weights were measured among dissections. The amount of starting material for tissue lysis was weighed to include approximately 30 mg of tissue per sample. All samples were lysed with TissueLyser II (Qiagen) in presence of one 5 mm stainless steel bead (Qiagen, Cat#: 69989) per sample. Tumor and muscle tissue samples were lysed two times for 2 min at 20 Hz and 30 Hz, respectively. All RNA was extracted with RNeasy[®] plus Universal Mini Kit (Qiagen, Cat#: 73404) according to the manufacturer's instruction protocol. Final concentrations and purity of RNA was measured with NanoDrop ND-1000 spectrophotometer. Tumor RNA-integrity was qualitatively

assessed with agarose gel electrophoresis: RNA quality was considered sufficient in samples with detectable bands for 18S and 28S ribosomal RNA (data not shown). cDNA was synthesized from RNA with the iScript™ Adv. cDNA Kit for RT-qPCR (Bio-Rad, Cat#: 172-5038) and RT-PCR was conducted with Eppendorf Thermal Cycler. The protocol used was 42°C for 30 min and 85°C for 5 min. From the tumor tissues, 2000 ng of template per sample was transcribed due to a high yield of RNA, whereas 1000 ng was transcribed from each muscle tissue sample.

qPCR was conducted for all samples with CFX96 Real-Time PCR apparatus (Bio-Rad) for Mstn, Activin-A and IL-6, as well as the calibrator genes Rn18S (tumor and muscle) and 36B4 (muscle). The qPCR protocol is shown in *Table 2*.

The qPCR products were analyzed for length with agarose gel electrophoresis for each gene from pooled samples for each tissue (the resulting gel is shown in supplementary data, *Appendix 2*).

Table 2: qPCR protocol used throughout this thesis. Denaturation, annealing and extension steps were run in 45 cycles. Pre-denaturation (in blue) was conducted only at the start of the protocol.

Step	Temperature	Time
Pre-denaturation	95°C	10 min
Denaturation	95°C	10 sec
Annealing	60°C	30 sec
Extension	72°C	30 sec

3.1.3 RT-qPCR data analysis

Initial cycle threshold (Ct) values were obtained from CFX-manager software and further processed with Microsoft excel. Ct-values for tumor and muscle samples were averaged from technical triplicates and duplicates, respectively. In technical triplicates, if the relative standard deviation of the Ct-values exceeded 2 %, the sample furthest from the mean was discarded. In technical duplicates, Samples with a relative Ct-standard deviation exceeding 2 % were removed from the analysis. These exclusion

criteria were omitted in IL-6 for muscle tissue and Mstn for tumor tissue due to high Ct-values and consequent high variance. In addition, samples associated with an abnormal melting point were discarded ($> 0.5C^{\circ}$ from the melting point of standard samples) in all cases. RT-qPCR expression values were obtained from the relative amount of transcript as in *Equation 1*, and normalized to the arithmetic mean of control group expression values for fold-change as in *Equation 2*. In the cases of tumor Mstn and muscle IL-6, expression data was transformed to a binary variable (amplification vs. no amplification, see statistical analysis).

$$\text{Equation 1: } \Delta Ct = 2^{-(Ct(\text{calibrator gene}) - Ct(\text{gene of interest}))}$$

$$\text{Equation 2: } \Delta\Delta Ct = \frac{\Delta Ct}{\text{mean}\Delta Ct(\text{control})}$$

3.2 C2C12 myoblast cell experiments

3.2.1 Thawing and cultivation of C2C12 cells

C2C12 cells (a gift from Dr. Riikka Kivelä, originally from ATCC) were obtained from $-150^{\circ}C$ freezer, thawed in $37^{\circ}C$ water bath, and seeded on two 75 cm^2 flasks with Dulbecco's Modified Eagle Medium (Gibco, Lot: 1715728) supplemented with 10% FBS (Gibco, Lot: 42Q1165K) and 1% penicillin/streptomycin. Cells were incubated in $37^{\circ}C$ 5% CO_2 and subcultured before confluency at 60 000 – 80 000 cells per flask until the last experiment. The passage number was between 6 and 9 throughout this study.

3.2.2 Optimization of C2C12 transfection

3.2.2.1 Transfection with Lipofectamine 3000 and Fugene 6

C2C12 and HepG2 (positive control) cells were seeded on a 24-well plate at a density of 7000 cells per cm^2 , 16 wells per cell line. At approximately 70% confluency, six wells for each cell line and each transfection reagent were transfected with a pGL3-CAGA₁₂-luciferase reporter plasmid (kindly provided by Dr. Arja Pasternack and Dr. Olli Ritvos, University of Helsinki. For details on the construct, see (Kaivo-Oja et. al.,

2005), with Protocol A (with commercially available Fugene 6 (Promega, Lot: 0000116983) and Protocol B (with commercially available Lipofectamine 3000 reagent, a gift from Dr. Varpu Marjomäki for the first experiment). Reaction conditions for all transfection protocols conducted in this work are shown in *Table 2*. As a negative control, throughout this study, mock transfection was conducted in an identical manner without the DNA-construct. Transfection vesicles were created with both reagents by incubating the gene construct with the reagent in Dulbecco's Modified Eagle Serum without additives for 15 min. Cells were incubated with the transfection vesicles for 6 h at 37°C in 5% CO₂. After the 6h incubation, one volume of medium with 20% FBS was added and incubation was continued overnight at 37 °C 5% CO₂. On the following day, medium was replaced for all wells and incubated overnight at 37°C 5% CO₂. Finally, medium was removed and 100 µl of 1X Passive Lysis Buffer was added to each well, followed by a 30-minute incubation shaking at room temperature. From each well, 10 µl of the produced lysate was transferred to optical white polystyrene 96-well plate (Thermo Fischer Scientific, Nunc coated, Lot: 1101260). Finally, 40 µl of Luciferase Assay Substrate (Promega, Lot: 0000025465) was added to each well and luciferase activity was immediately quantified with Promega Glomax[®] luminometer.

Table 2: Protocol transfection conditions.

Protocol	Reagent	Amount of reagent (volume %)	DNA-construct (ng/ μ l)
A	Fugene 6	0.12	0.1
B	Lipofectamine 3000	0.15	1
C	Lipofectamine 3000	0.15	2
D	Lipofectamine 3000	0.3	1
E	Lipofectamine 3000	0.3	2

3.2.2.2 Optimization of Lipofectamine 3000 transfection

Cells were seeded at a density of 15000 cells per cm^2 on an optical white 96-well plate. On the following day (at approximately 70% confluency), cells were transfected with four different protocols: B, C, D and E ($n = 5$, see *Table 2* for protocol details). For each protocol, the transfection reagent (Thermo Fischer Scientific, 1810834) and DNA-construct were incubated 15 min RT. After incubation, wells were washed with PBS and transfection mixes were introduced to the wells. After 6h at 37°C in 5% CO_2 incubation, one volume of medium with 20% FBS was added to the wells, and incubation was continued at 37°C (5% CO_2) overnight. On the following day, cells were washed with PBS and media was replaced with 0.2% FBS DMEM and incubated for 4h at 37°C in 5% CO_2 . After incubation, cells were introduced to 10 ng/ml of crude Activin-A (15 $\mu\text{g/ml}$, produced in CHO-S cells at the University of Helsinki by Dr. Arja Pasternack. Concentration is approximated from activity analysis against a purified preparate) and incubated overnight at 37°C in 5% CO_2 . After 24 h incubation, 1 volume of britelite Plus Reporter Gene Assay System reagent (PerkinElmer, Lot:

110-16401) was added to each well and luciferase activity was quantified with Promega Glomax[®] luminometer.

3.2.2.3 Further optimization of Lipofectamine 3000 transfection

Cells were seeded at a density of 17000 cells per cm² on a 96-well plate, and transfected on the following day (at approximately 85% confluency) with protocol E with and without P3000[™] reagent (Thermo Fischer Scientific, Lot#: 1824474) ($n = 5$). The transfection steps and luciferase activity measurement were conducted as previously described.

3.2.3 Exposure to Activin-A and ACVR2B

3.2.3.1 Activin-A exposure

Cells were seeded and transfected with protocol E + P3000[™] as previously described. On the third day, cells were exposed to 0, 25, 50 and 100 ng/ml Activin-A for 24h ($n = 5$). Luciferase activity was measured as previously described.

3.2.3.2 ACVR2B ligand blockade

Cells were seeded and transfected with protocol E + P3000[™] as previously described. On the third day, all wells were exposed to 25 ng/ml Activin-A. In one group, wells were additionally exposed to 1:1 mass ratio (25 ng/ml) of sACVR2B ($n = 5$) produced by Arja Pasternack as explained elsewhere (Hulmi et. al., 2013). Luciferase activity was measured as previously described.

3.3 Statistical analysis

RT-qPCR data was assessed for normality with visual methods (Q-Q plots) and Shapiro-Wilk's test, and further analyzed with Mann-Whitney U or One-Way ANOVA (Student's *t*-test for post hoc comparisons, due to robustness for unequal variance) based on normality assumptions. In the cases of muscle IL-6 and tumor Mstn, statistical analysis was conducted with Chi-squared tests.

All luciferase assay data was analyzed with One-Way ANOVA and Student's *t*-tests. Due to a small sample-size, normal distribution of the luciferase assay

experiments was assumed based on earlier studies conducted with similar methodology (Dzieran et. al., 2013; Lin et. al., 2005). $P < 0.05$ was considered statistically significant. IBM® SPSS® Statistics (v. 24) was used for all statistical analyses.

4. RESULTS

4.1 Basic characteristics of the tumour-bearing mice

LLC tumours did produce fat cachexia, but not significant muscle wasting. Instead, C26 tumour produced a large decrease in both skeletal muscle and fat mass (Nissinen et. al., 2016).

4.2 Relative expression levels in tumor

Rn18S calibrator gene Ct-values were not statistically significantly different in C26 and LLC (see supplementary data, *Appendix 3*). The relative expression levels of ActA (*Inhba*) and IL-6 were both significantly higher in C26-tumors when compared to control (LLC-tumor). Mean fold-change for ActA and IL-6 were 87 and 262, respectively. The aforementioned expression levels are shown in Fig. 2.

Mstn was amplified in 87.5 % and 12.5 % of samples in C26 and LLC groups, respectively ($\chi^2 = 9.0$, $df = 1$, $P < 0.01$), indicating that Mstn is generally expressed in C26, but not in LLC-tumors.

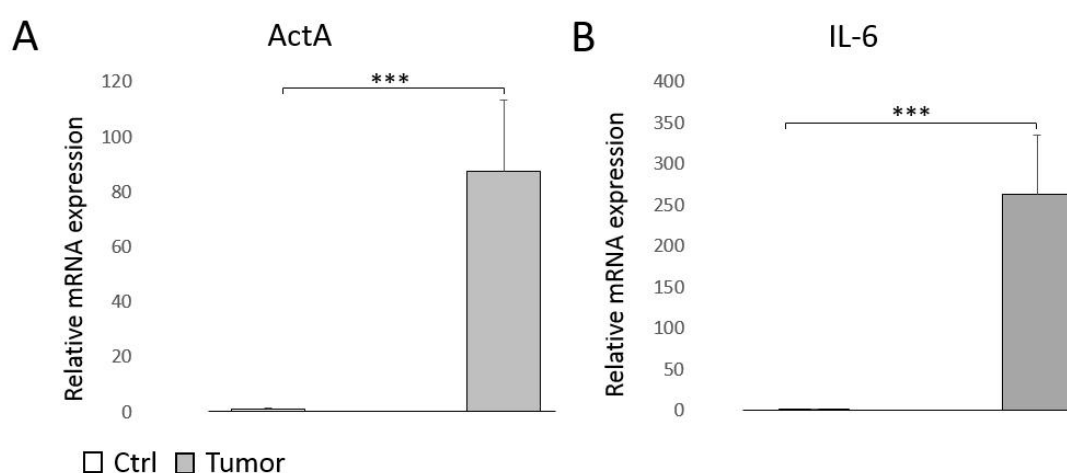


Figure 2: Relative expression of ActA and IL-6 in mouse C26 and LLC tumors. A) Mean ActA expression in C26 tumor tissue is 87-fold relative to LLC. B) Mean IL-6 expression in C26 tumor tissue is 262-fold relative to LLC. *** $P < 0.001$ (One-Way ANOVA for A ActA and Mann-Whitney U for IL-6)

4.3 Relative expression levels in muscle

Rn18S calibrator gene Ct-values were not statistically significantly different between the groups (see supplementary data, *Appendix 3*). ActA expression levels were lower in the test groups. Mean fold-change for ActA was 0.43 for C26 + PBS and 0.40 for C26 + sACVR2B ($P < 0.05$). The changes observed in Mstn were not statistically significant. The relative expression levels for muscle ActA and Mstn are shown in Fig. 3.

IL-6 was amplified in 28.6 % and 75 % of samples in control and C26 + PBS groups, respectively. The resulting chi-squared statistic was borderline statistically significant ($\chi^2 = 4.67$, $df = 1$, $P = 0.051$).

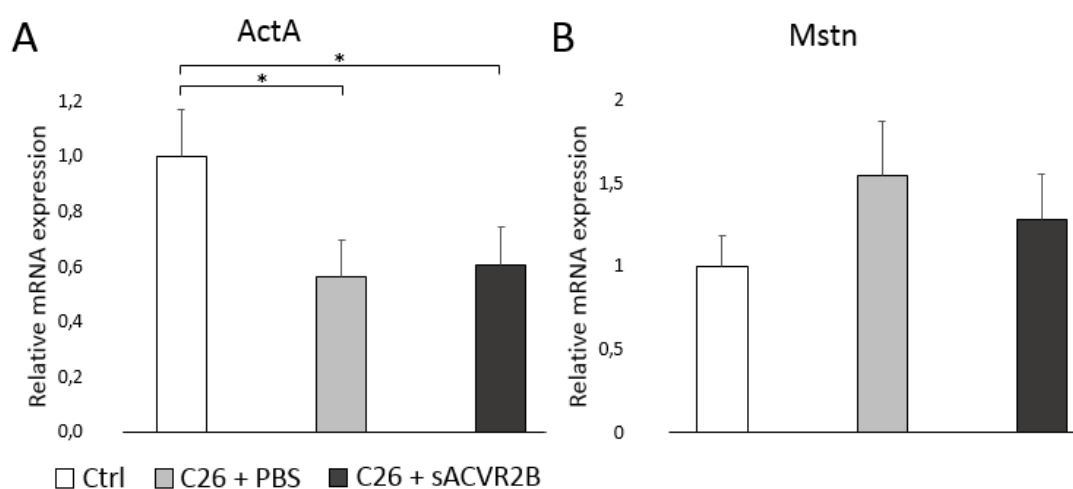


Figure 3: Relative expression levels of ActA and Mstn in mouse gastrocnemius muscle. A) Results show a statistically significant reduction in mean ActA expression in C26 + PBS and C26 + sACVR2B groups relative to control. B) One-Way ANOVA did not indicate a statistically significant difference between the groups. * $P < 0.05$ (One-Way ANOVA)

4.4 Lipofectamine 3000 and Fugene 6 Reagents in C2C12 Transfection

Lipofectamine 3000 transfection of C2C12-cells resulted in a statistically significantly higher luciferase activity compared to negative control ($P < 0.001$), and also gave a stronger mean signal than the transfection of HepG2-cells with Fugene 6 (positive control, a previously proved to work protocol with HepG2). Initial transfection results with Lipofectamine 3000 and Fugene 6 are shown in Fig. 4.

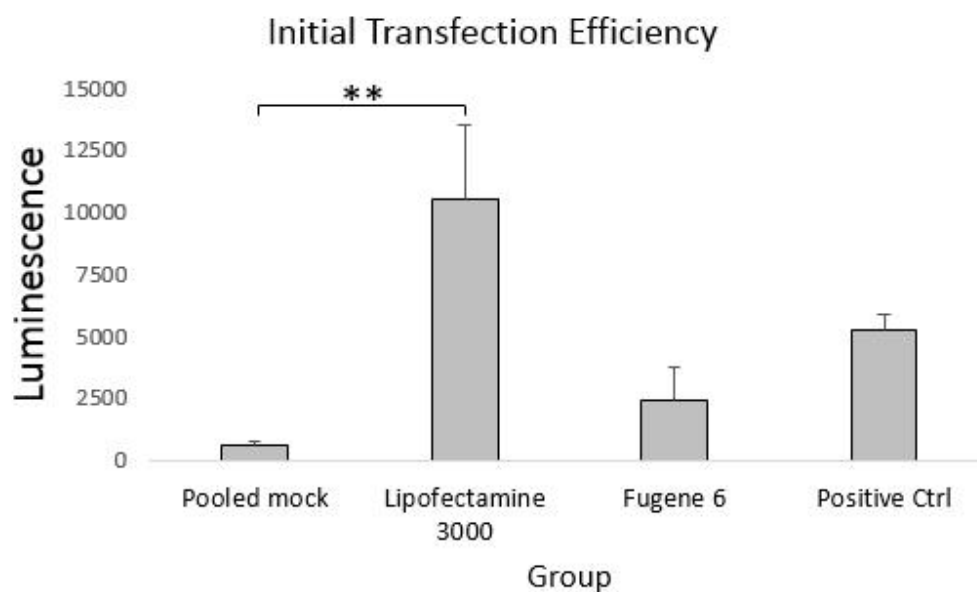


Figure 4: Initial transfection efficiencies for C2C12-cells with Lipofectamine 3000 and Fugene 6. HepG2-cells with Fugene 6 transfection was used as a positive control. Lipofectamine 3000 produced the best signal and was chosen for further optimization. ** $P < 0.01$

4.5 Optimization of Lipofectamine 3000 transfection

Protocol C increased luminescence signal 4.2-fold from the negative control, and protocol E further improved luciferase activity to 9.3-fold ($P = 0.018$ and 0.006 , respectively). Transfection results for different protocols are shown in Fig. 5 A. The effect of P3000™ reagent to transfection efficiency for protocol E is shown in Fig. 5 B.

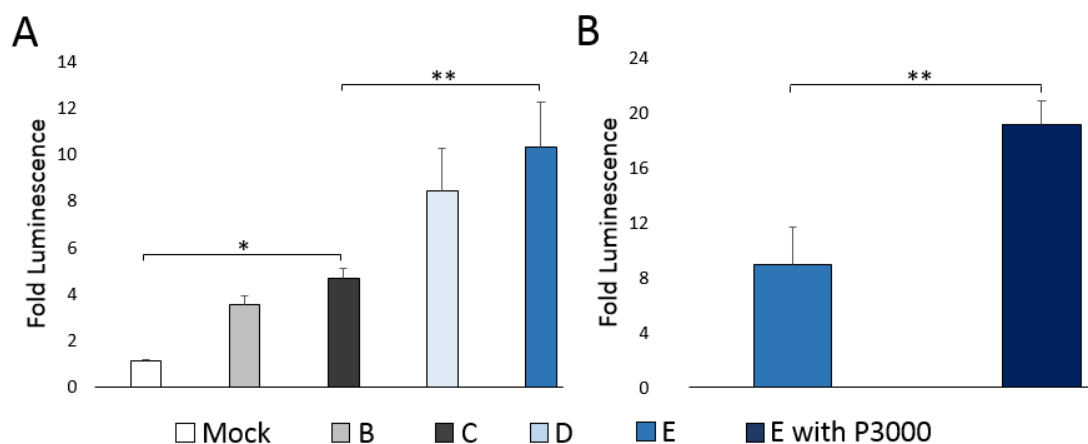


Figure 5: Transfection efficiencies for the conducted transfection protocols with C2C12-cells and Lipofectamine 3000. A) Protocol E produced the highest luciferase activity. B) The P3000 reagent provided with Lipofectamine 3000 further increased luciferase activity by approximately 2-fold. * $P < 0.05$ ** $P < 0.01$

4.6 Activin-A exposure and blockade

Administration of 25 ng/ml ActA into the growth medium increased luciferase activity by 3.9-fold compared to the untreated group ($P < 0.001$). Dosage of over 25 ng/ml did not further increase luciferase activity at a statistically significant level. ActA blockade with 1:1 mass-ratio sACVR2B resulted in an 4-fold decrease in signal compared to the untreated group. The concentration gradient exposure response and blockade of 25 ng/ml ActA with 1:1 sACVR2B are shown in fig. 6 and fig. 7, respectively.

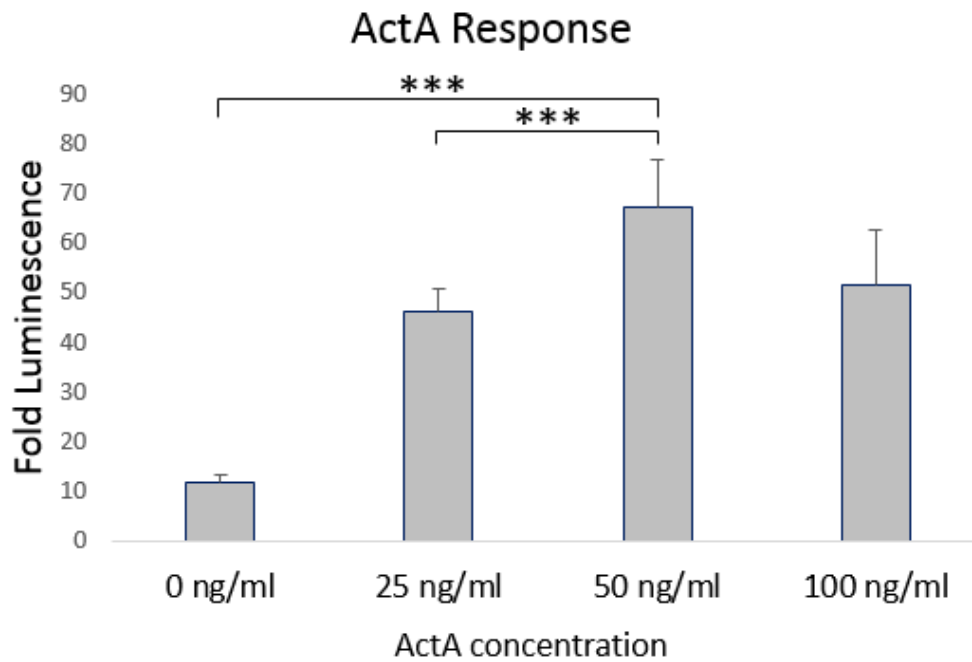


Figure 6: Response in luminescence for ActA dosage. 25 ng/ml of ActA produced a statistically significant increase in signal. The increase from mean endogenous (0 ng/ml) to exogenous (25 ng/ml) signal is 3.9-fold. All the groups differed statistically significantly from mock and 0 ng/ml, but statistical difference was not observed between 25, 50 and 100 ng/ml. *** $P < 0.001$

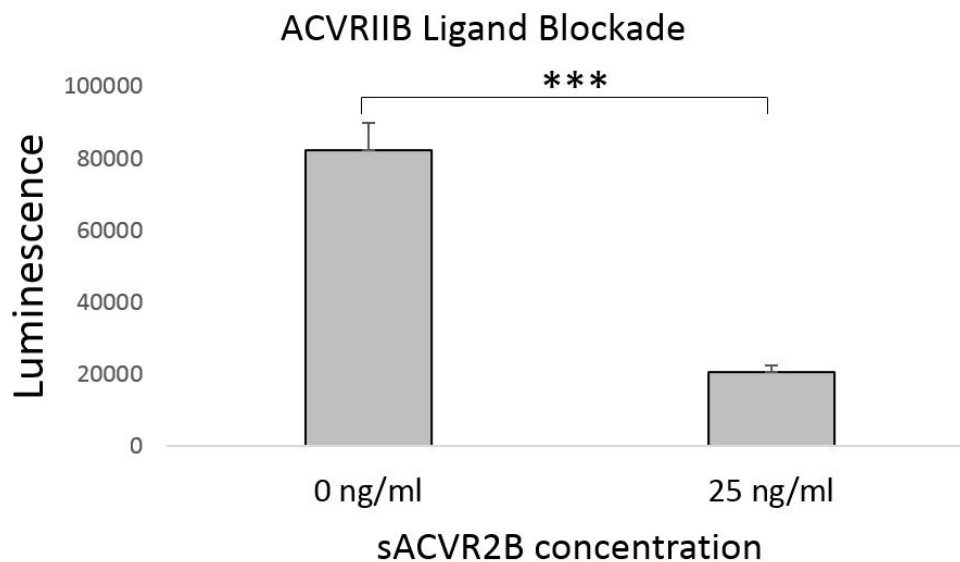


Figure 7: sACVR2B blockade of 25 ng/ml exogenous ActA. An 1:1 mass-ratio of sACVR2B vs. ActA reduced signal 4-fold compared to endogenous derived activity (0 ng/ml). *** $P < 0.001$

5. DISCUSSION

5.1 Tumor and muscle gene expression levels

The purpose of this work was to assess the expression levels of the cachectic factors in the relevant tissues, tumor and muscle. ActA gene was expressed at a significantly higher level in C26-tumor when compared to LLC-tumor. In skeletal muscle ActA gene was expressed lower in C26-tumor-bearing mice muscle (with and without treatment) compared to control. Tumor ActA overexpression has previously been shown to be associated with increased tumor progression, and its circulating levels correlate with muscle wasting. (Chen et. al., 2014; Okano et. al., 2013) In this regard, the results imply that tumor derived ActA may contribute to muscle wasting in C26 induced CAC. To confirm this, the magnitude of secreted ActA should be assessed from C26-conditioned medium with non-cachectic controls, and assess the individual effect of this biomarker to muscle growth *in vitro*, or to explicitly block or silence ActA *in vivo*. Since the sACVR2B-treatment did not restore the level of ActA expression in muscle, it seems unlikely that receptor binding TGF- β protein superfamily members are responsible for this effect. Since ActA is a negative regulator of muscle mass, the lowered mRNA-levels in muscle are not likely relevant regarding CAC-symptoms, but rather a side effect arising from the metabolic chaos, or an inadequate protective mechanism against muscle atrophy. The lowered expression of ActA in muscle shown in this thesis differed from an earlier observation in a similar setting, where muscle ActA mRNA levels were unaffected by the tumor (Zhou et. al., 2010). The result by Zhou et. al. is open for question, since the underlying data was not shown in the publication. Nevertheless, it has been indicated that the tumor inoculation site and microenvironment, as well as C26 storage conditions and passage number have effects on the secreted mediators of CAC and consequently the severity of cachectic symptoms, implying that the results are prone to variation (Matsuyama et. al., 2015). Moreover, the timing of tissue collection to 11 days after tumor inoculation may show different effects compared to earlier or later time-points.

Mstn expression was higher in the cachectic C26 tumor, but overall physiological importance may be negligible based on high Ct-values: difference in

mean Ct-values between Mstn and ActA in C26 accounts for over 1400-fold abundance in ActA, if equal efficiency is assumed for both transcripts. However, quantitative analysis for fold-expression was not possible because of censored data points (no amplification in PCR, likely due to negligible amount of transcript). Thus, the evidence of the contribution of circulatory C26-tumor secreted Mstn to CAC remains elusive, although the relatively low amount of transcript raises doubt about its significance. Consequently, the presence and amount of secreted Mstn should be assessed from C26 conditioned medium and specifically silenced in CAC-producing *in vivo* tumors to clarify the issue further. Nevertheless, systemic Mstn secreting CHO-tumors are sufficient to induce muscle wasting. (Zimmers et. al., 2002) Thus, multiple different mechanisms could contribute to the phenomena.

Studies have shown increased Mstn expression levels in the cachetic skeletal muscle, which backs up its role as a paracrine factor in CAC in the muscle tissue environment (Zhou et. al., 2010; Costelli et. al., 2008). Although this thesis failed to show a statistically significant increase in Mstn expression in the skeletal muscle of the tumor-bearing group, this was mainly because of insufficient statistical power ($1-\beta = 0.3$), and the direction of the effect was fitting in both study groups (increased in C26, and alleviated with treatment). Additionally, the assessment of paracrine regulation should include expression analyses of other contributing factors, such as Mstn inhibitors and ACVR2B. For instance, Follistatin, an Mstn inhibitor, also plays a role in CAC (Costelli et. al., 2008). A variable derived from multiple contributing factors would likely improve the effect size and, consequently, statistical power. The combined effect of these factors would give a more clarified picture of the CAC phenomena and the symptom-alleviating downstream effectors of sACVR2B-treatment.

IL-6 was markedly overexpressed in the tumor, which is in accordance with earlier studies (Lonnroth et. al., 1994). C26 cells secrete IL-6 to the surrounding environment and the magnitude of the mRNA-level correlates with circulating concentration. (Norden et. al., 2015) Elevated IL-6 expression in cancer cells promotes tumor proliferation, survival and formation of metastases. In CAC, elevated serum concentration of IL-6 has been documented, and it drives body mass and adipose tissue

loss, as well as synergistic skeletal muscle wasting in combination with other cachectic factors such as ActA. (Chen et. al., 2016) All in all, elevated IL-6 mRNA observed in the tumors is in accordance with earlier experiments conducted with the C26 cell line. Interestingly, IL-6 expression was also generally observed in muscle tissue of the tumor-bearing group (observed in 6 out of 8) while it was under the detection limit in most of the control group samples (observed in 2 out of 7) ($P = 0.051$). In the muscle tissue environment, IL-6 may have tissue protective effects. (Belizario et. al., 2016; Serrano et. al., 2008) Possibly, this expression pattern is a host mechanism to repair the CAC induced damage. This result should however be revised with more sensitive methods such as digital PCR, due to the scarce amount of transcript present in the tissues.

Neither of the calibrator genes were statistically significantly different between the groups (see supplementary data, *Appendix 3*), suggesting that they were suitable for normalization. In the tumor calibrator gene, the mean Ct-value was higher in the C26-group. Thus, even if the calibrator difference would manifest bias, the calculated differences would be underestimates and therefore the statistics are reliable. In the muscle calibrator gene, 36B4, the slight differences in the mean Ct-values could theoretically overestimate and underestimate the differences in ActA and Mstn, respectively. Due to the slight difference observed in mean calibrator Ct-values, an additional calibrator gene run was conducted for the muscle samples in attempt to improve accuracy. The second gene, Rn18S, manifested greater differences in the same direction as 36B4. The Ct-values in the 36B4 and Rn18S correlated strongly ($R^2 = 0.84$, $P < 0.001$). Thus, it is likely that the observed difference emerges from variance in the total concentration arising from the RNA-preparation and reverse transcriptase steps. Normalization of these factors is the ultimate goal in using calibrator genes, and in this regard, the results can be considered reliable (Kozera and Rapacz, 2013). 36B4 was ultimately chosen as calibrator for the muscle samples due to a lower within and between groups variation. Overall, both tumor and muscle calibrator genes performed as desired.

It has been speculated that the CAC-inducing factors arise to release nutrients like amino acids and lipids into the bloodstream to be utilized by the tumor. In this

regard, increased expression and secretory activity of tumoral factors leading to muscle and adipose tissue wasting would directly improve tumor growth and proliferation. (Porporato, 2016) However, this alone does not improve the fitness of a certain CAC-inducing clonal neoplastic cell population, but rather the whole tumor (Greaves and Maley, 2012). Therefore, these factors, if present, are likely so from the progenitor stage of the cancer lifecycle, or alternatively, evolve with properties that promote a more efficient utilization of the circulating nutrients. From this viewpoint, CAC-inducing factors should be associated with increased cancer aggressiveness and poor survival, which is indeed the case at least with tumor ActA overexpression (Okano et al., 2013). This nutrient-based hypothesis could also partly explain the prolonged survival achieved by inhibiting muscle-wasting factors, such as ActA and Mstn with sACVR2B: the cancer has less nutrients to fuel its growth. In the test groups of this study, treatment did not however affect tumor size at a statistically significant level (data not shown), which partly contradicts this reasoning. The evolutionary perspective should nonetheless be considered when studying the causality of events concerning CAC: how does cachectic factors such as ActA and IL-6 promote tumor progression and increased aggressiveness, and do atrophic events in skeletal muscle reflect selective advantages in the tumor environment?

5.2 Optimization of C2C12 transfection

The aim of the transfection experiments was to create a functional transfection protocol with the CAGA-luciferase gene construct for the C2C12 cell line. The reagent of choice for transfection optimization was Lipofectamine 3000 based on the initial result, where Lipofectamine was statistically significantly different from negative control and showed a better mean response in luminescence compared to the positive control group. C2C12 transfection failed completely with the initial protocol for Fugene 6, since ActA administration did not affect its signal (data not shown). Protocol E resulted in the highest luminescence signal, which was further improved with the P3000™ reagent provided with Lipofectamine 3000 (it. The general trend was that a higher concentration of the DNA-construct or transfection reagent resulted in an improved signal. However, further increasing the concentrations from protocol E

caused marked cytotoxicity and consequently resulted in higher variance of signal between the wells, albeit mean signal was also increased (see supplementary data, *Appendix 4*). A possible explanation for the increased signal and the marked increase in variance is that while a larger proportion of the viable cells possibly contained the gene construct, the proportion of viable cells varied significantly between the wells due to the toxic effect. It is noteworthy, that the CAGA-luciferase DNA-construct is not constitutively active, but rather dependent of Smad signaling and thus in the presence of endogenic or exogenic TGF- β proteins. Albeit endogenous TGF- β activity also produces a detectable signal, 10 ng/ml of ActA was used as a constant concentration in all of the transfection protocols to amplify the signal from background luminescence.

The C2C12 myoblast cell line is notoriously transfection resistant, which is a major factor hindering its use in research (Liang et. al., 2016). This work presents a successful optimized transfection protocol, which can be utilized in further research concerning C2C12 myoblast cells. It should be noted, that the luminescence signal measured with the Glomax[®] luminometer does not measure absolute transfection efficiency (i.e. % of cells containing the gene-construct), but signal strength can be used to compare relative efficiencies of the different protocols. The aim was to develop a protocol with high signal-to-background ratio and low variance between samples to be able to detect group differences with reasonable sample sizes. For this, the presented protocol serves its purpose.

One drawback in using the transfected C2C12-cells is that they are in the myoblast form, and therefore not completely analogous to mature muscle cells. The C2C12-myoblasts can be differentiated to myotubes with appropriate conditions, but it is unclear whether the transfected gene construct would still be present after differentiation, and this issue should be tested subsequently. However, cachexia also induces effects to muscle progenitor cells, and these effects can be studied with myoblasts (He et. al., 2013). Indeed, muscle tissue is a heterogeneous system, and this should be taken into account when studying the effects of cachetic mediators *in vitro* (He et. al., 2013)

5.3 C2C12 ActA exposure and blockade

Administration of 25 ng/ml ActA elevated luciferase activity 3.85-fold from endogenous derived activity. Concentration of 1:1 (25 ng/ml) sACVR2B reduced luciferase activity by 4-fold. This implies that the exogenous effect was completely blocked with the employed concentration. Although the result from 0 to 25 ng/ml ActA administration and 0 to 25 ng/ml blockade are from separate experiments and cannot thus be statistically analyzed, the downward fold-change is even higher in the case of sACVR2B-blockade (albeit ideally the blockade would have needed an additional control with analogous transfection and 0 ng/ml ActA). Increase in ActA concentration to 50 or 100 ng/ml did not produce significant increase in signal. Possibly, in C2C12-cells, the ACVR2B-receptors are already saturated at lower concentrations, and concentrations exceeding 50 ng/ml encompasses apparent cytotoxic effects. The concentrations applied in this thesis are not meant to be optimal in studying the effect of ActA in CAC, but rather to indicate that ActA administration to C2C12 cells results in a detectable amplified signal, and that sACVR2B treatment eliminates this effect. The transfected CAGA-luciferase plasmid can be utilized when studying the effects of any TGF- β protein, with affinity for ACVR2B, to C2C12 cells. Additionally, this assay can be used to measure the TGF- β protein activity of different cell-line conditioned media (e.g. cachetic vs. non-cachetic). The effects of these TGF- β proteins on the expression of downstream effectors as well as protein synthesis and degradation rates would be subsequent intrinsic research prospects.

REFERENCES

- Amirouche, A., A.C. Durieux, S. Banzet, N. Koulmann, R. Bonnefoy, C. Mouret, X. Bigard, A. Peinnequin, and D. Freyssenet. 2009. Down-regulation of Akt/mammalian target of rapamycin signaling pathway in response to myostatin overexpression in skeletal muscle. *Endocrinology*. 150:286-294.
- Aoyagi, T., K.P. Terracina, A. Raza, H. Matsubara, and K. Takabe. 2015. Cancer cachexia, mechanism and treatment. *World J.Gastrointest.Oncol*. 7:17-29.
- Aversa, Z., A. Bonetto, F. Penna, P. Costelli, G. Di Rienzo, A. Lacitignola, F.M. Baccino, V. Ziparo, P. Mercantini, F. Rossi Fanelli, and M. Muscaritoli. 2012. Changes in myostatin signaling in non-weight-losing cancer patients. *Ann.Surg.Oncol*. 19:1350-1356.
- Belizario, J.E., C.C. Fontes-Oliveira, J.P. Borges, J.A. Kashiabara, and E. Vannier. 2016. Skeletal muscle wasting and renewal: a pivotal role of myokine IL-6. *Springerplus*. 5:619-016-2197-2. eCollection 2016.
- Bertram, J.S., and P. Janik. 1980. Establishment of a cloned line of Lewis Lung Carcinoma cells adapted to cell culture. *Cancer Lett*. 11:63-73.
- Bonetto, A., J.E. Rupert, R. Barreto, and T.A. Zimmers. 2016. The Colon-26 Carcinoma Tumor-bearing Mouse as a Model for the Study of Cancer Cachexia. *J.Vis.Exp.* (117). doi:10.3791/54893.
- Chen, J.L., K.L. Walton, H. Qian, T.D. Colgan, A. Hagg, M.J. Watt, C.A. Harrison, and P. Gregorevic. 2016. Differential Effects of IL6 and Activin A in the Development of Cancer-Associated Cachexia. *Cancer Res*. 76:5372-5382.
- Chen, J.L., K.L. Walton, C.E. Winbanks, K.T. Murphy, R.E. Thomson, Y. Makanji, H. Qian, G.S. Lynch, C.A. Harrison, and P. Gregorevic. 2014. Elevated expression of activins promotes muscle wasting and cachexia. *FASEB J*. 28:1711-1723.
- Corbett, T.H., D.P. Griswold Jr, B.J. Roberts, J.C. Peckham, and F.M. Schabel Jr. 1975. Tumor induction relationships in development of transplantable cancers of the colon in mice for chemotherapy assays, with a note on carcinogen structure. *Cancer Res*. 35:2434-2439.
- Costelli, P., M. Muscaritoli, A. Bonetto, F. Penna, P. Reffo, M. Bossola, G. Bonelli, G.B. Doglietto, F.M. Baccino, and F. Rossi Fanelli. 2008. Muscle myostatin signalling is enhanced in experimental cancer cachexia. *Eur.J.Clin.Invest*. 38:531-538.
- Ding, H., G. Zhang, K.W. Sin, Z. Liu, R.K. Lin, M. Li, and Y.P. Li. 2016. Activin A induces skeletal muscle catabolism via p38beta mitogen-activated protein kinase. *J.Cachexia Sarcopenia Muscle*.
- Dzieran, J., J. Fabian, T. Feng, C. Coulouarn, I. Ilkavets, A. Kyselova, K. Breuhahn, S. Dooley, and N.M. Meindl-Beinker. 2013. Comparative analysis of TGF-beta/Smad signaling dependent cytoskeleton in human hepatocellular carcinoma cell lines. *PLoS One*. 8:e72252.
- Fearon, K., F. Strasser, S.D. Anker, I. Bosaeus, E. Bruera, R.L. Fainsinger, A. Jatoi, C. Loprinzi, N. MacDonald, G. Mantovani, M. Davis, M. Muscaritoli, F. Ottery, L. Radbruch, P. Ravasco, D. Walsh, A. Wilcock, S. Kaasa, and V.E. Baracos. 2011. Definition and classification of cancer cachexia: an international consensus. *Lancet Oncol*. 12:489-495.
- Fearon, K.C., D.J. Glass, and D.C. Guttridge. 2012. Cancer cachexia: mediators, signaling, and metabolic pathways. *Cell.Metab*. 16:153-166.

- Gilson, H., O. Schakman, S. Kalista, P. Lause, K. Tsuchida, and J.P. Thissen. 2009. Follistatin induces muscle hypertrophy through satellite cell proliferation and inhibition of both myostatin and activin. *Am.J.Physiol.Endocrinol.Metab.* 297:E157-64.
- Giri, D., M. Ozen, and M. Ittmann. 2001. Interleukin-6 is an autocrine growth factor in human prostate cancer. *Am.J.Pathol.* 159:2159-2165.
- Greaves, M., and C.C. Maley. 2012. Clonal evolution in cancer. *Nature.* 481:306-313.
- Gu, H., Y. Cao, B. Qiu, Z. Zhou, R. Deng, Z. Chen, R. Li, X. Li, Q. Wei, X. Xia, and W. Yong. 2016. Establishment and phenotypic analysis of an Mstn knockout rat. *Biochem.Biophys.Res.Commun.* 477:115-122.
- Han, H.Q., X. Zhou, W.E. Mitch, and A.L. Goldberg. 2013. Myostatin/activin pathway antagonism: molecular basis and therapeutic potential. *Int.J.Biochem.Cell Biol.* 45:2333-2347.
- Hatakeyama, S., S. Summermatter, M. Jourdain, S. Melly, G.C. Minetti, and E. Lach-Trifilieff. 2016. ActRII blockade protects mice from cancer cachexia and prolongs survival in the presence of anti-cancer treatments. *Skelet Muscle.* 6:26-016-0098-2. eCollection 2016.
- He, W.A., E. Berardi, V.M. Cardillo, S. Acharyya, P. Aulino, J. Thomas-Ahner, J. Wang, M. Bloomston, P. Muscarella, P. Nau, N. Shah, M.E. Butchbach, K. Ladner, S. Adamo, M.A. Rudnicki, C. Keller, D. Coletti, F. Montanaro, and D.C. Guttridge. 2013. NF-kappaB-mediated Pax7 dysregulation in the muscle microenvironment promotes cancer cachexia. *J.Clin.Invest.* 123:4821-4835.
- Hedayati, M., Z. Nozhat, and M. Hannani. 2016. Can the Serum Level of Myostatin be Considered as an Informative Factor for Cachexia Prevention in Patients with Medullary Thyroid Cancer? *Asian Pac.J.Cancer.Prev.* 17 Spec No.:119-123.
- Hulmi, J.J., B.M. Oliveira, M. Silvennoinen, W.M. Hoogaars, H. Ma, P. Pierre, A. Pasternack, H. Kainulainen, and O. Ritvos. 2013. Muscle protein synthesis, mTORC1/MAPK/Hippo signaling, and capillary density are altered by blocking of myostatin and activins. *Am.J.Physiol.Endocrinol.Metab.* 304:E41-50.
- Kaivo-Oja, N., D.G. Mottershead, S. Mazerbourg, S. Myllymaa, S. Duprat, R.B. Gilchrist, N.P. Groome, A.J. Hsueh, and O. Ritvos. 2005. Adenoviral gene transfer allows Smad-responsive gene promoter analyses and delineation of type I receptor usage of transforming growth factor-beta family ligands in cultured human granulosa luteal cells. *J.Clin.Endocrinol.Metab.* 90:271-278.
- Kozera, B., and M. Rapacz. 2013. Reference genes in real-time PCR. *J.Appl.Genet.* 54:391-406.
- Lee, S.J., and A.C. McPherron. 2001. Regulation of myostatin activity and muscle growth. *Proc.Natl.Acad.Sci.U.S.A.* 98:9306-9311.
- Liang, R., W. Dong, X. Shen, X. Peng, A.G. Aceves, and Y. Liu. 2016. Modeling Myotonic Dystrophy 1 in C2C12 Myoblast Cells. *J.Vis.Exp.* (113). doi:10.3791/54078.
- Lin, A.H., J. Luo, L.H. Mondschein, P. ten Dijke, D. Vivien, C.H. Contag, and T. Wyss-Coray. 2005. Global analysis of Smad2/3-dependent TGF-beta signaling in living mice reveals prominent tissue-specific responses to injury. *J.Immunol.* 175:547-554.
- Lonnroth, C., J. Gelin, and K. Lundholm. 1994. Expression of interleukin-6 in tumor-bearing mice with cytokine dependent cachexia. *Int.J.Oncol.* 5:329-336.

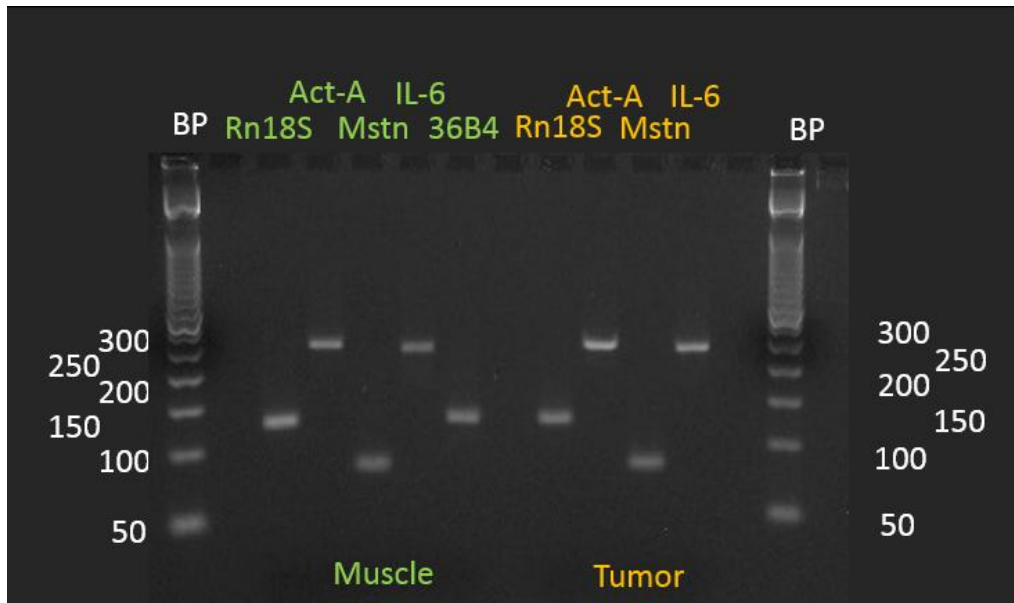
- Maddocks, M., J. Hopkinson, J. Conibear, A. Reeves, C. Shaw, and K.C. Fearon. 2016. Practical multimodal care for cancer cachexia. *Curr.Opin.Support.Palliat.Care*.
- Matsuyama, T., T. Ishikawa, T. Okayama, K. Oka, S. Adachi, K. Mizushima, R. Kimura, M. Okajima, H. Sakai, N. Sakamoto, K. Katada, K. Kamada, K. Uchiyama, O. Handa, T. Takagi, S. Kokura, Y. Naito, and Y. Itoh. 2015. Tumor inoculation site affects the development of cancer cachexia and muscle wasting. *Int.J.Cancer*. 137:2558-2565.
- McPherron, A.C., A.M. Lawler, and S.J. Lee. 1997. Regulation of skeletal muscle mass in mice by a new TGF-beta superfamily member. *Nature*. 387:83-90.
- Miyamoto, Y., D.L. Hanna, W. Zhang, H. Baba, and H.J. Lenz. 2016. Molecular Pathways: Cachexia Signaling-A Targeted Approach to Cancer Treatment. *Clin.Cancer Res*. 22:3999-4004.
- Nissinen, T.A., J. Degerman, M. Rasanen, A.R. Poikonen, S. Koskinen, E. Mervaala, A. Pasternack, O. Ritvos, R. Kivela, and J.J. Hulmi. 2016. Systemic blockade of ACVR2B ligands prevents chemotherapy-induced muscle wasting by restoring muscle protein synthesis without affecting oxidative capacity or atrogenes. *Sci.Rep*. 6:32695.
- Norden, D.M., R. Devine, D.O. McCarthy, and L.E. Wold. 2015. Storage Conditions and Passages Alter IL-6 secretion in C26 adenocarcinoma cell lines. *MethodsX*. 2:53-58.
- Okano, M., H. Yamamoto, H. Ohkuma, Y. Kano, H. Kim, S. Nishikawa, M. Konno, K. Kawamoto, N. Haraguchi, I. Takemasa, T. Mizushima, M. Ikeda, T. Yokobori, K. Mimori, M. Sekimoto, Y. Doki, M. Mori, and H. Ishii. 2013. Significance of INHBA expression in human colorectal cancer. *Oncol.Rep*. 30:2903-2908.
- Petruzzelli, M., and E.F. Wagner. 2016. Mechanisms of metabolic dysfunction in cancer-associated cachexia. *Genes Dev*. 30:489-501.
- Porporato, P.E. 2016. Understanding cachexia as a cancer metabolism syndrome. *Oncogenesis*. 5:e200.
- Rozen, S., and H. Skaletsky. 2000. Primer3 on the WWW for general users and for biologist programmers. *Methods Mol.Biol*. 132:365-386.
- Sartori, R., G. Milan, M. Patron, C. Mammucari, B. Blaauw, R. Abraham, and M. Sandri. 2009. Smad2 and 3 transcription factors control muscle mass in adulthood. *Am.J.Physiol.Cell.Physiol*. 296:C1248-57.
- Sato, N., M.C. Michaelides, and M.K. Wallack. 1981. Characterization of tumorigenicity, mortality, metastasis, and splenomegaly of two cultured murine colon lines. *Cancer Res*. 41:2267-2272.
- Serrano, A.L., B. Baeza-Raja, E. Perdiguero, M. Jardí, and P. Muñoz-Canoves. 2008. Interleukin-6 is an essential regulator of satellite cell-mediated skeletal muscle hypertrophy. *Cell.Metab*. 7:33-44.
- Tan, C.R., P.M. Yaffee, L.H. Jamil, S.K. Lo, N. Nissen, S.J. Pandol, R. Tuli, and A.E. Hendifar. 2014. Pancreatic cancer cachexia: a review of mechanisms and therapeutics. *Front.Physiol*. 5:88.
- Temel, J.S., A.P. Abernethy, D.C. Currow, J. Friend, E.M. Dues, Y. Yan, and K.C. Fearon. 2016. Anamorelin in patients with non-small-cell lung cancer and cachexia (ROMANA 1 and ROMANA 2): results from two randomised, double-blind, phase 3 trials. *Lancet Oncol*. 17:519-531.
- Thissen, J.P., and A. Loumaye. 2013. Role of Activin A and Myostatin in cancer cachexia. *Ann.Endocrinol.(Paris)*. 74:79-81.

- Tisdale, M.J. 2009. Mechanisms of cancer cachexia. *Physiol.Rev.* 89:381-410.
- Tsuchida, K., M. Nakatani, K. Hitachi, A. Uezumi, Y. Sunada, H. Ageta, and K. Inokuchi. 2009. Activin signaling as an emerging target for therapeutic interventions. *Cell.Commun.Signal.* 7:15-811X-7-15.
- Yaffe, D., and O. Saxel. 1977. Serial passaging and differentiation of myogenic cells isolated from dystrophic mouse muscle. *Nature.* 270:725-727.
- Ye, J., G. Coulouris, I. Zaretskaya, I. Cutcutache, S. Rozen, and T.L. Madden. 2012. Primer-BLAST: a tool to design target-specific primers for polymerase chain reaction. *BMC Bioinformatics.* 13:134-2105-13-134.
- Zhou, X., J.L. Wang, J. Lu, Y. Song, K.S. Kwak, Q. Jiao, R. Rosenfeld, Q. Chen, T. Boone, W.S. Simonet, D.L. Lacey, A.L. Goldberg, and H.Q. Han. 2010. Reversal of cancer cachexia and muscle wasting by ActRIIB antagonism leads to prolonged survival. *Cell.* 142:531-543.
- Zimmers, T.A., M.V. Davies, L.G. Koniaris, P. Haynes, A.F. Esquela, K.N. Tomkinson, A.C. McPherron, N.M. Wolfman, and S.J. Lee. 2002. Induction of cachexia in mice by systemically administered myostatin. *Science.* 296:1486-1488.

SUPPLEMENTARY DATA

Appendix 1: All tested primer sequences. Sequences marked in red did not pass the initial criteria for proper function: Mstn_2 had a non-linear standard curve, and GDF15 had two peaks in sample melting curves, proposing primer-dimer formation. GDF15 also a prominent CAC-biomarker which was initially included, but was discarded from this study because of time constraints.

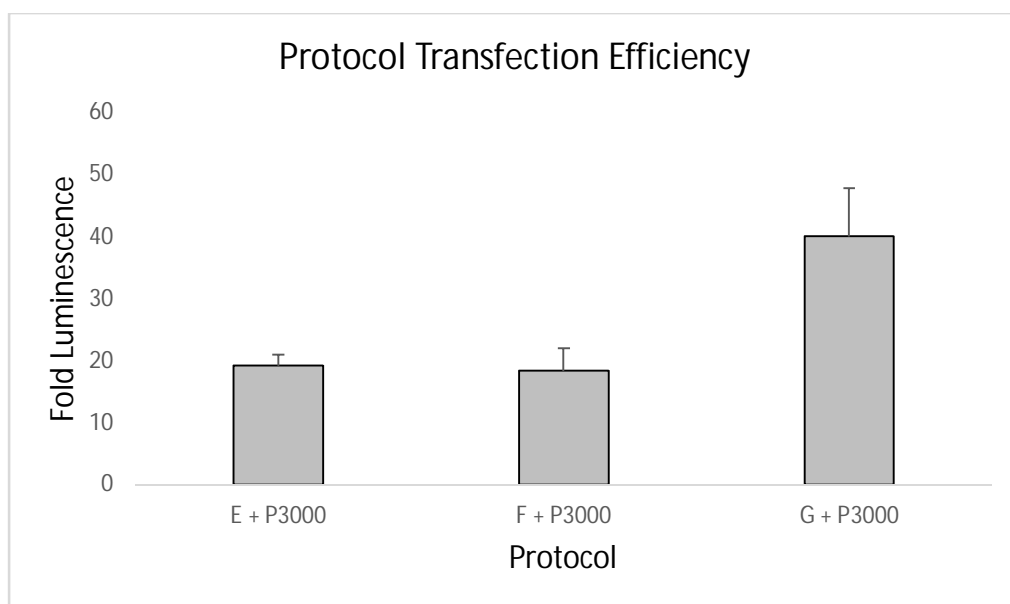
Primer	Sequence (5' → 3')
Mstn_1F	AAGATGGGCTGAATCCCTTT
Mstn_1R	GCAGTCAAGCCCAAAGTCTC
Activin-A_1F	GAACGGGTATGTGGAGATAG
Activin-A_1R	TGAAATAGACGGATGGTGAC
IL-6_1F	ATTCCAGAAACCGCTATGAA
IL-6_1R	CCATTGCACAACCTTTTTCT
Rn18S_F1	GCAATTATTCCCCATGAACG
Rn18S_R1	GGCCTCACTAAACCATCCAA
36B4_F1	GGCCCTGCACTCTCGCTTTC
36B4_R1	TGCCAGGACGCGCTTGT
IL-6_R2	CTGATGCTGGTGACAACCAC
IL-6_F2	CAGAATTGCCATTGCACAAC
Mstn_F2	CTACCACGGAAACAATCATTACCA
Mstn_R2	GTTTCAGAGATCGGATTCCAGTAT
GDF15_F1	CACTGCAGACTTATGATGAC
GDF15_R1	AAATACACAATCCATCCACC



Appendix 2: DNA-electrophoresis gel from pooled samples of muscle and tumor qPCR-runs. All of the RT-qPCR products align at the correct product size axis. Expected product sizes (bp): Rn18S: 124; ActA: 240; IL-6:230; Mstn: 80; 36B4: 124. All the products are located at their expected sites.

Appendix 3: Calibrator gene Ct means, standard deviations and P-values for muscle 36B4 (green), muscle Rn18S and tumor Rn18S (orange) groups. There were no statistical differences among the groups. Since the muscle 36B4 and Rn18S correlate strongly ($R^2 = 0.84$, $P < 0.001$), the mean differences likely arise from concentration differences between the samples.

Group	Ct-mean	SD	S_{bet}	P
Muscle Ctrl	21.75	0.50	0.45	0.20
Muscle C26	22.65	0.95	-	-
Muscle C26 + sACVR2B	22.20	1.11	-	-
Muscle Ctrl	15.09	1.11	0.65	0.28
Muscle C26	16.41	1.54	-	-
Muscle C26 + sACVR2B	15.73	1.70	-	-
Tumor C26	12.40	0.80	0.57	0.09
Tumor LLC	11.60	0.96	-	-



Appendix 4: Transfection efficiencies for the highest concentration protocols. Protocol F: 0.6 % Lipofectamine 3000 and 2 ng/ μ l CAGA; Protocol G: 0.6 % Lipofectamine 3000 and 4 ng/ μ l CAGA. The increase in variance was observed with increased cytotoxicity for protocol F and G, although the mean signal was improved in protocol G. Increasing concentrations further was therefore not conducted, and protocol E + P3000 was regarded as best performing.